The Rock Varnish in the Messak Settafet (Fezzan, Libyan Sahara), Age, Archaeological Context, and Paleo-Environmental Implication

Mauro Cremaschi

C.N.R., Centro di Studio Geodinamica Alpina e Quaternaria, Dipartimento di Scienze della Terra, via Mangiagalli 34, 20133 Milan, Italy

The manganese-rich rock varnish from the Messak Settafet plateau is a relict feature that developed at the end of the Holocene humid cycle, before the onset of the present-day hyperarid conditions. The Messak Settafet varnish consists of three microlayers of different composition and micromorphological features. The innermost microlayer is composed of illuvial clay. The second, middle microlayer is the classic manganese-rich rock varnish. The outermost microlayer is composed of unaltered aeolian dust. Each microlayer formed under different climatic conditions, and the microstratigraphy records a climatic evolution from a wet environment towards progressivé desertification. The relationship between desert varnish, rock engravings, and radiocarbon-dated archaeological evidence and the comparison with the Holocene climatic evolution as from cave deposits suggest that most of the varnish developed since the end of the VI millennium B.P. under a semiarid climate characterized by steppe-type vegetation, up to the onset of desert conditions, during the IV millennium B.P.

INTRODUCTION

Rock varnish is a manganese-rich black patina which covers vast extensions of barren rock in dry environments (Cooke et al., 1993). Modern analytical techniques such as electron microscope and microprobe analyses have been essential to understanding that the desert varnish does not consist of material drawn in solution from the rock underneath and precipitated by evaporation, but of wind blown dust subsequently enriched in situ by manganese (Potter and Rossman, 1977; Allen, 1978). Biochemical processes associated with bacteria and perhaps fungi are reputed to be the main agents in fixing and concentrating manganese (Dorn and Oberlander, 1981a), which can be replaced or enhanced, in some cases, by physicochemical process (Jones, 1991).

In any case, formation of the varnish requires well-constrained ecological settings. It will not form if the environment is too humid and Eh fluctuates widely, since manganese-fixing bacteria are outcompeted by moss, lichens, or other epilithic organisms (Dorn, 1984, 1990; Dorn, 1994; Jones, 1991; Oberlander, 1994). Moreover, the environment should not be too arid because high

Geoarchaeology: An International Journal, Vol. 11, No. 5, 393–421 (1996)
 CCC 0883-6353/96/050393-29

alkalinity and pH, for instance, in addition to wind-blown alkaline dust, inhibit bacterial growth (Dorn and Oberlander, 1981b).

In many deserts, formation of rock varnish occurs today; many believe that varnish cannot survive long enough to be an indicator of past climatic conditions (Cooke et al., 1993). In contrast, in the central Sahara where manganese-rich varnish is related to the oldest assemblages of the rock engravings representing a wild savanna fauna and large cattle (Graziosi, 1942; Jelinek, 1985; Castiglioni and Negro, 1986) whose subsistence is incompatible with the present extreme aridity.

This article discusses the nature of central Saharan varnish, its environmental and archaeological implications, and whether Saharan varnish can act as a useful tool to reconstruct the desert environments of the past.

GENERAL SITE INFORMATION

The Messak Settafet is located in Fezzan (Libya) (Figure 1). It is a NE–SW trending plateau, from Ubari to the Tehi-n-Aghelad pass, consisting of continental sandstone of Jurassic to Cretaceous age (Nubian sandstones). Messak Sattafet has a mean elevation of about 700 m a.s.l. The present climate of the area is hyperarid, with a mean annual precipitation of 10 mm and a mean annual temperature of 22.5°C in Murzuq (Walter and Lieth, 1960).

GEOMORPHOLOGICAL SETTING

The dominant landscape of the Messak plateau is a vast, black hamada. The brilliant and light-colored substrate is thoroughly stained by black varnish a few microns-thick. This dominant blackness is characteristic for the Messak Settafet, even in small-scale satellite photographs, and gives the area its name. Settafet in the Targhi language means "black."

At the top of the plateau, which is the relict of a tertiary pediment (Bushe, 1980; Cremaschi, 1994), black varnish coats all the landscape features: clasts resting on the bedrock, as well as all Paleolithic and Neolithic artifacts and megaliths. However, only the part of both stones and artifacts that emerge from the soil is coated by manganese-rich desert varnish. In contrast, the buried stone surfaces exhibit a brilliant reddish color.

The plateau is dissected by deep canyons developed since the Middle Pleistocene. The canyons are inactive today, but the wadi beds at their base are occupied by large gravel bars which are probably Late Pleistocene in age as they include Aterian stone artifacts (Cremaschi, 1944).

The manganese-rich desert varnish coats both the surfaces of the cliffs—including some of the petroglyphs depicted on them—and the fluvial bars at their base. It is lacking, however, under the shelters and in cave porches. The transition between coated and uncoated surfaces occurs by means of interfingering varnish streaks, indicating that occasional rain showers enhance the formative processes of the coating.

Along the wadis, cliff surfaces are at present subjected to intense degradational processes. The surfaces that have been exposed recently by rock collapse are not covered by the manganese-rich desert varnish and exhibit a reddish patina. Wide rock outcrops are also stripped of the varnish as a result of wind abrasion. The surfaces still covered by the black varnish, however, are crosscut by a network of uncoated fractures, which developed after the formation of the black varnish.

The varnish-coated surfaces are being dismantled by the geomorphological processes which are active in the area. Consequently, the black manganese-rich coating, which I refer to as desert varnish, does not seem to be forming at present and appears to be a relict geomorphologic feature.

SAMPLING AND ANALYTICAL TECHNIQUES

The field characteristics of the varnish appear to be similar in all the areas that have been surveyed between the pass of Tehi-n-Aghelad, wadi In Elobu, wadi Matendush, and Bir Taziet. Five sampling localities were selected as representative of the whole area (Figure 1), and 60 samples were collected to represent all the different geomorphologic units on which the varnish occurs and the archaeological artifacts of different ages (rock engravings and radiocarbon-dated archaeological stone structures). The samples from rock engravings were taken from vertical cliffs, homogeneously covered by black varnish. In order to avoid the possible influence of spatial variability, all samples were collected at the rock art station of In-Habeter (25°45′53″N; 12°10′49″E), where all the stylistic groups are represented (Graziosi, 1942). In order to avoid injury to the engravings, samples were as small as possible, exploiting by natural breakages. All the varnish samples came from sandstone with similar lithologic characteristics.

Micromorphological observations were made both from thin sections using a conventional petrographic microscope and with a Cambridge 100 scanning electron microscope (SEM) using secondary electrons. Subsequently, an energy dispersive X-ray analyzer (EDAX) connected to the SEM was utilized to identify the varnish components. SEM analyses were performed on carbon-coated polished sections cut perpendicular to the varnish surface; 89 sections and 2234 individual micron-scale analyses were taken. All elemental concentrations are reported as oxide weights normalized to 100%.

MICROMORPHOLOGICAL CHARACTERISTICS

The color of the varnish is 5YR (4/1 (dark gray) (Munsell Soil Color Charts), whereas the color of the unaltered rock ranges from 5YR 6/6 (reddish yellow) to 5YR 5/4 (reddish brown). Sedimentologically, the local sandstone is a medium-grained quartz arenite, commonly medium grain size. Clasts both on the top of the hamada and on the cliffs exhibit, on the microscopic scale, a rough surface with protruding quartz grains. SEM observations of the surfaces of

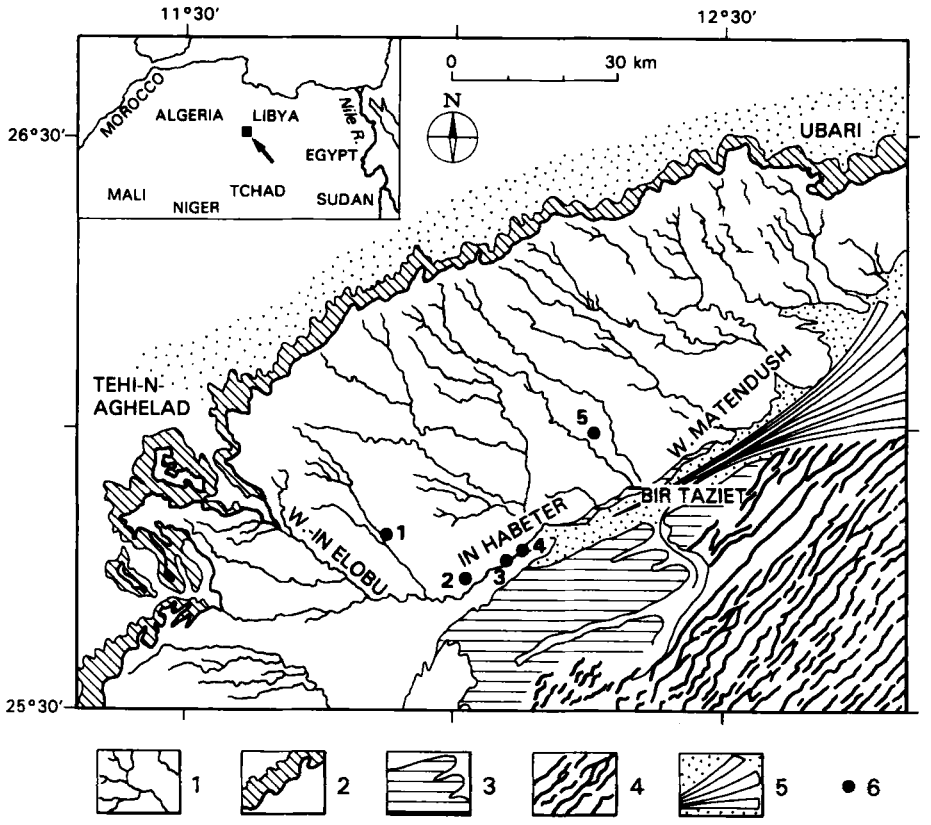

Figure 1. Schematic physiographic map of the Messak Settafet. **1.** Hamada and hydrographic net; **2.** pediment; **3.** oxisol terrace; **4.** erg and interdune dry lakes; **5.** Matendush alluvial fan. **6.** Location of sampling sites: (1) Wadi Tilizzagen; (2) Matendush cave; (3) In-Habeter archaeological site and rock art station; (4) sampled toposequence at In-Habeter; (5) In Aghalas site (IHA).

clasts reveal that the black varnish commonly fills depression pits between quartz grains and thus smooths the rock surface (Figure 2). The varnish infills contain, in some cases, particles of external provenance, such as pollen grains and allocthonous coccoliths.

EDAX analysis of the varnish surface has revealed that it consists mostly of Mn- and Fe-rich components. The distribution of manganese and iron is not homogeneous at the surface of the sample as they are found mostly in intergranular depressions and can be totally lacking at the top of quartz grains. Consequently, observed in cross-section, the varnish is discontinuous. It thickens in the intergranular pits, and can be completely absent at the top of the largest quartz grains. In the pits, where the varnish is thicker (Figure 3), it typically consists of three microlayers, lying on the bedrock. From the outer surface (Figure 4):

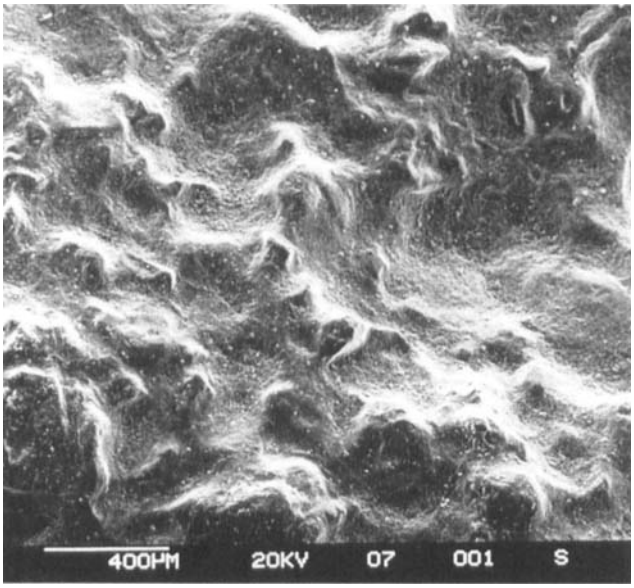

Figure 2. SEM image of the surface of the Fe-Mn-rich varnish: The topography of the quartz grains is smoothed by the varnish components, which bridge grains on the subaerial surface.

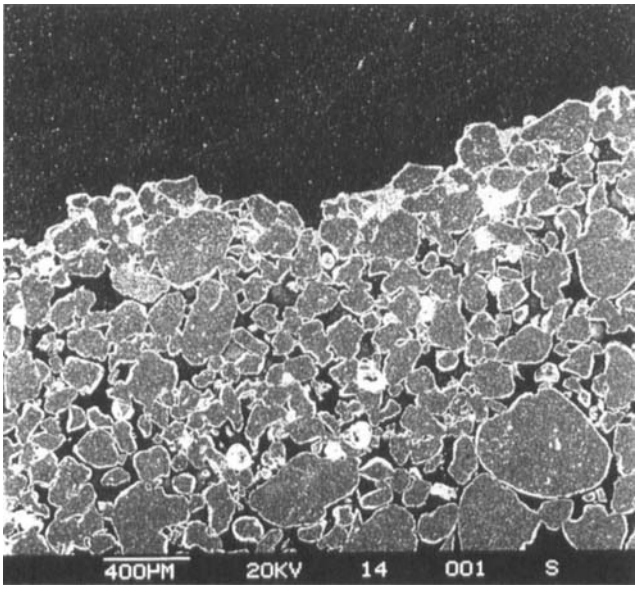

Figure 3. Cross section of the Fe-Mn-rich varnish imaged with secondary electrons: Close to the surface, intergranular spaces are filled by varnish material to a thickness of about 100–200 μm.

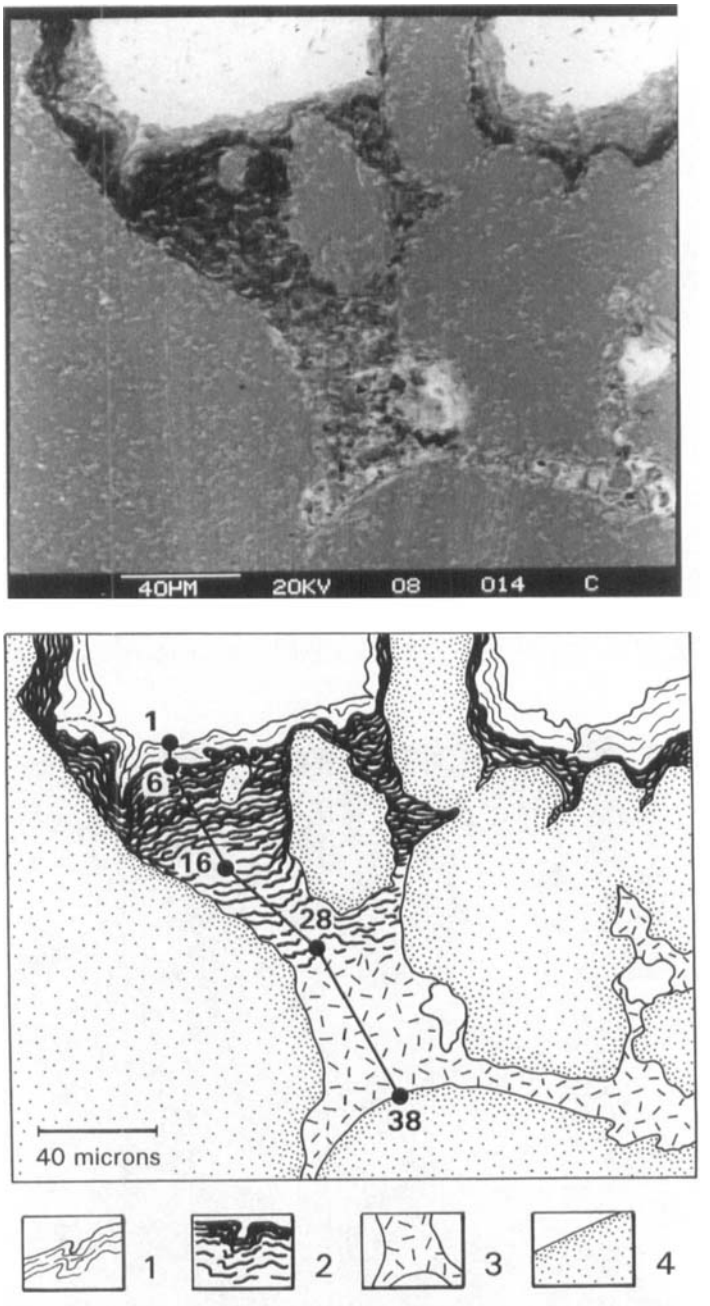

Figure 4. Cross section of the Fe-Mn-rich varnish in inverted backscattered electron microscopy (sample 14 A6; the location of the analyzed points is indicated; EDAX chemical transect in Fig. 8). The microlayer 2 appears black in inverted backscatter. (1) microlayer 1; (2) microlayer 2; (3) microlayer 3; (4) quartz grains.

1. **The outer microlayer.** Under the optical microscope this microlayer is light colored and birefringent in crossed polarized light, and pale in inverted backscattered mode with the SEM. Its maximum thickness ranges from 10 to 30 μm with a well-defined median at about 20 μm. It is thinly laminated. The laminae are lenticularly organized or often convoluted. In some cases they contain detrital components such as quartz grains and angular to subrounded reworked fragments of black varnish (microlayer 2) transported from the sides of the microdepression. As the outermost, and fragile in consistence, the outer microlayer breaks and is the first to be removed by erosion.
2. **The opaque, black middle microlayer.** This microlayer appears dark under inverted backscattered electron imaging and consists of undulated lenticular laminae. Its maximum thickness ranges from 25 to 80 μm, with smooth median at about 60 μm. When it is particularly developed, the top of the microlayer is massive and thick, while the lamination becomes progressively more distinctive towards the bottom. This layer is the main one responsible for the dark visual color of the varnish, and it corresponds to the classical manganese-rich rock varnish as described in the literature.
3. **The innermost microlayer.** Under the SEM this microlayer is characterized by large clay crystals arranged in an apparently disordered fabric. Clay minerals fill intergranular voids, apparently without any preferential pattern. Clay minerals fill all the intergranular pores to a depth of 600 μm from the surface and then progressively decrease and disappear. Observations with the optical microscope revealed that this microlayer consists of birefringent, occasionally microlaminated red clay coatings (Figure 5). Towards the top, the clay has a porphyric related distribution, whereas towards the bottom the distribution is chitonic (terminology from Bullock et al., 1985). Small calcium carbonate nodules with irregular surfaces are interspersed within the clay; they exhibit low interference colors. This microlayer is generally discontinuous and is absent in sections observed in the more recent hosts such as Neolithic artifacts and megalithic monuments.
4. **Bedrock.** Bedrock consists of subrounded to rounded, clast-supported, medium-size quartz, some of which display evidence of overgrowths. The voids are about the 25% of the whole area of the sample. Bedrock grains are occasionally coated by thin discontinuous coatings of weakly birefringent clay; they are more developed at the top of the microlayer and gradually disappear towards the base. In the samples in which the microlayer 3 does exist, a 1-mm-thick reduction rim has been observed, at a depth of 4–5 mm. The reduction rim is parallel to the surface, and the sandstone is more friable and bleached above it.

CHEMICAL COMPOSITION

The composition of the Messak varnish is similar to that discussed in the literature (Oberlander, 1994). Silicon, Al, Fe, Mg, Ca, Mg, Ba, Na, K, and P are the major components of varnish with subordinate amounts of S and Cl.

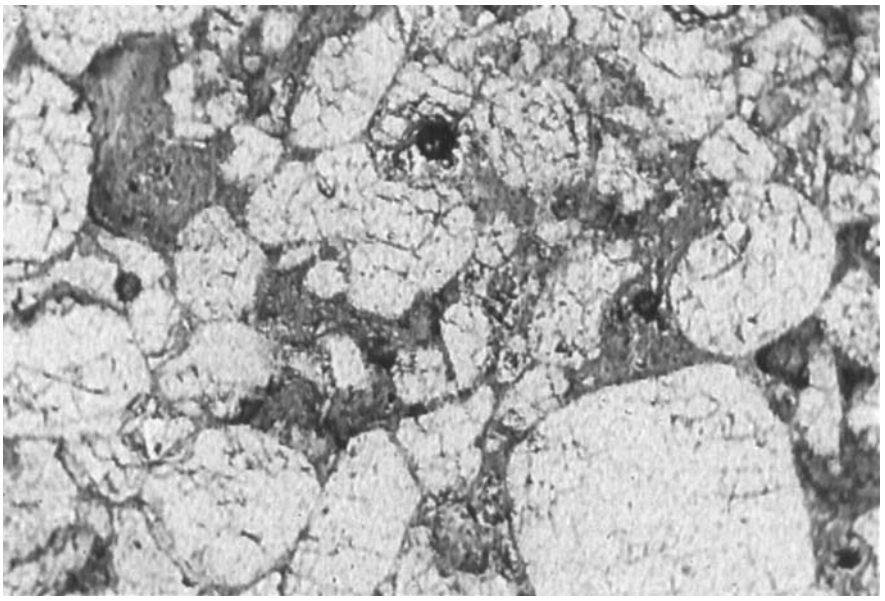

Figure 5. The microlayer 3 in thin section (sample BUBA): microlaminated red cutans fill intergranular voids (100, PPL).

Silicon and Al occur as components of illite-montmorillonite clay minerals; single peaks of Si are indicative for quartz dust; Fe and Mn occur as (hydrous) oxides. Calcium is present alone as a component of calcium carbonate which has been observed also in thin section as concretions or coatings. Most frequently Ca and P systematically display a parallel trend, which may indicate that the two ions combined to form calcium phosphate minerals, which have been also recorded in some Californian varnishes (Reneau et al., 1992). Sulfur in some cases is positively correlated with Ca indicating gypsum as in the lower sample of the In-Habeter cairn. More frequently S concentrations correspond to peaks of Ba and indicate the occurrence of barium sulfate, probably barite ($BaSO_4$), which has been recorded in many cases in desert varnish (Krinsley, et al., 1990; Reneau et al., 1992).

The chemical composition of the varnish is rather different, in both quantity and incidence of the elements, from that of the clay cement occurring discontinuously on the quartz grains of the parent material. The cement consists of weakly birefringent clay composed of Si (SiO_2 from 70% to 99%) and subordinate Al (Al_2O_3 from 1% to 28%). Phosphorus, Ca, Mg, K, and Ba rarely reach up to 1%; iron is present in minor amounts, and Mn is almost lacking.

Each microlayer, identified by the micromorphological analysis, displays a different chemical composition. Sample IHA was collected on a flat varnish-coated surface in the center of the plateau along wadi In Aghalas (IHA) (25°

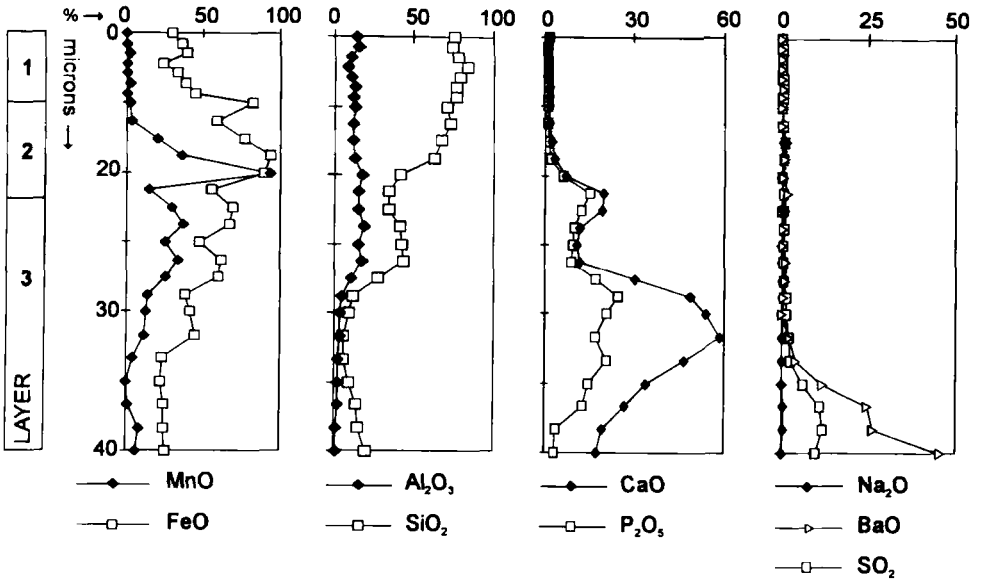

Figure 6. The chemical transect of the IHA sample. Microlayers are indicated in the left column.

59′50″N; 12°16′55″E) and serves as an example of the general EDAX chemical composition in Figure 6 and in Table I. The uppermost microlayer 1 is homogeneous and consists predominantly of Si, Al and minor amounts of Fe, whereas the more soluble elements (Ca, Na) are almost lacking. Microlayer 2 is Mn- and Fe-rich and the Mn/Fe ratio varies from 1.2 to 8, with median value 3.5. Calcium and P gradually increase with depth. The third microlayer is composed of a heterogeneous admixture of elements; Fe and Mn, while decreasing in respect of the upper horizon, are still present, but they are not connected to a laminated fabric as in microlayer 2. Clay mineral content generally increases, but in the case of the IHA P and Ca are rather high, and show a clear peak at the base of the microlayer. As P and Ca gradually increase with depth, it seems likely that their distribution is a function of leaching from the upper part of the varnish and of postdepositional concentration at its base. Barium and S display a similar trend as they gradually increase with depth and show an high concentration in layer 3. As barite is rather mobile, it may have been leached and reprecipitated at the base of the varnish section. However, in most of the cases discussed here Ba-S concentrations are included in layer 2 and display a positive correlation with Mn peaks.

The chemical analyses are represented graphically (Figure 6) where some parameters selected as meaningful for the reconstruction of the formation processes are plotted as a function of depth. The Mn and Fe oxides are presented alone, and in some cases compared with Mn/Fe ratio in order to emphasize Mn concentrations.

Table I. EDAX chemical analyses (spot size 1 μm) of the IHA sample along the chemical transect as in Figure 6.

	Layer 1							Layer 2					
pts	*1*	*2*	*3*	*4*	*5*	*6*	*7*	*8*	*9*	*10*	*11*	*12*	*13*
μ	0.0	1.4	2.9	4.3	5.7	7.1	8.6	10.0	12.5	15.0	17.5	20.0	22.5
SiO_2	75.47	74.20	78.08	82.99	78.48	76.11	77.04	70.61	72.92	67.45	61.99	41.56	34.29
Al_2O_3	13.64	15.08	10.95	8.82	10.82	13.31	11.41	12.99	11.24	12.03	12.83	17.31	15.88
TiO_2	0.45	0.67	0.75	0.15	0.59	0.62	0.38	0.57	0.42	0.48	0.55	0.46	0.32
MnO	0.00	0.00	0.21	0.00	0.00	0.21	0.00	0.25	0.29	1.97	3.65	9.35	1.47
FeO	3.01	3.62	3.89	2.30	3.30	3.82	4.46	8.15	5.88	7.61	9.35	8.98	5.58
CaO	1.21	0.89	0.93	0.97	1.15	1.18	1.35	1.31	1.65	2.47	3.30	6.90	19.81
MgO	2.32	2.56	1.96	1.76	1.91	1.84	2.25	2.76	2.25	2.51	2.78	4.61	3.95
Na_2O	0.44	0.00	0.17	0.35	0.48	0.00	0.05	0.10	0.41	0.21	0.00	0.37	0.81
K_2O	1.40	1.46	1.30	0.91	1.26	1.39	1.43	1.86	1.78	2.26	2.74	2.51	1.73
P_2O_5	1.25	1.12	1.15	1.05	1.01	0.86	1.14	1.07	1.00	1.44	1.88	6.04	15.23
ClO_2	0.57	0.25	0.53	0.35	0.42	0.38	0.19	0.05	0.20	0.23	0.25	0.09	0.38
SO_2	0.23	0.07	0.08	0.21	0.35	0.22	0.15	0.22	0.62	0.36	0.10	0.40	0.40
BaO	0.00	0.10	0.00	0.13	0.23	0.06	0.15	0.06	1.35	0.97	0.59	1.44	0.17
	100.00	100.00	100.00	100.00	100.00	100.00	100.00	99.98	100.00	99.99	99.98	100.01	100.00

	Layer 3													
pts	*14*	*15*	*16*	*17*	*18*	*19*	*20*	*21*	*22*	*23*	*24*	*25*	*26*
μ	23.0	24.0	25.0	26.5	27.0	28.5	30.0	32.5	34.5	36.0	37.5	39.0	40.0
SiO_2	33.89	40.61	41.98	43.52	26.92	11.74	8.94	6.13	6.46	8.86	13.96	15.83	19.66
Al_2O3	14.92	18.34	15.21	17.13	10.23	4.40	3.75	3.09	2.64	2.27	2.83	1.08	1.44
TiO_2	1.31	0.66	8.16	1.49	0.39	0.38	0.19	0.00	0.00	0.00	0.00	0.00	0.00
MnO	2.97	3.73	2.52	3.41	2.59	1.39	1.28	1.18	0.39	0.00	0.14	0.87	0.66
FeO	6.96	6.69	4.79	6.12	5.93	3.87	4.18	4.50	2.33	2.26	2.44	2.50	2.51
CaO	19.46	12.04	10.77	11.86	30.19	48.77	53.75	58.72	46.80	33.99	26.82	19.50	17.34
MgO	3.27	4.61	3.47	3.89	2.23	0.86	0.67	0.49	0.64	0.83	0.91	0.00	0.39
Na_2O	0.82	0.00	0.16	0.00	0.00	0.35	0.18	0.00	0.15	0.36	0.51	0.00	0.00
K_2O	2.43	2.13	1.75	2.19	2.63	1.41	1.55	1.69	0.97	1.04	0.97	0.99	0.77
P_2O_5	12.35	9.88	9.43	9.10	16.78	24.80	20.88	16.96	20.97	14.66	12.79	3.78	3.20
ClO_2	0.56	0.30	0.27	0.30	0.43	0.68	0.69	0.70	0.95	0.39	0.79	0.30	0.20
SO_2	0.82	0.52	0.25	0.34	1.37	1.21	1.92	2.62	5.96	10.88	11.94	9.62	6.27
BaO	0.24	0.51	1.25	0.65	0.27	0.14	2.03	3.92	11.75	24.46	25.92	45.55	47.57
	100.00	100.00	100.00	100.01	99.95	100.00	100.01	100.01	100.00	100.00	100.00	100.00	100.00

Silicon and Al are considered as representative of finely subdivided quartz and clay particles that are the most frequent components of the aerosol in the region (Coudé-Gaussen, 1991). Calcium together with P reaches high percentages. The origin of the P in this environment is still unclear. It could be derived from organic activity from the soils, from lichen activity at the surface of the rock (Syers and Iskandar, 1973), or from bird guano, and later combined with calcium present in the environment. The relict soils occurring at the top of the hamada include Ca in the form of carbonatic concretions. However, the primary source of Ca, which is completely absent from the parent material, may be lake deposits surrounding the Messak (Cremaschi, 1994). The lake deposits consist of caliche crusts and soft limestone that range in age from middle Pleistocene to Holocene. Gypsum and halite, which were the source for the S and Na included in the varnish, have been found only in the late Holocene lake deposits, as they were formed at the time of the lake's desiccation (Di Lernia and Cremaschi, in press) and were available to deflation only since this time. Barium exists in low percentages in the cement of the local sandstone, and it is absent or occurs in very slight amounts in the aeolian dust as recorded in layer 1. Similarly to Ca, the main source of Ba could be the relict soils at the top of the hamada. Combination barium with S—conducive to barite formation—may be an autochtonous process related to the development of the manganese-rich varnish development (Reneau et al., 1992).

A TOPOSEQUENCE OF VARNISH OUTCROPS

As the forming factors (rate of deposition of dust, moisture availability, leaching, evapotranspiration) are expected to change with topography, a toposequence of varnish outcrops has been sampled close to the rock art site at In-Habeter III in the left bank of the wadi Matendush (Figure 7). This sequence compares varnish developed on top of the hamada (sample 14A6), along the cliff (samples BHC3, BUBA, 6A), and on gravel of an inactive bar of the wadi (sample 5A). Thickness of the microlayers and chemical analyses of samples collected along this toposequence are indicated in Figure 8.

Along the topographic profile, the characteristics of the varnish are quite similar with regard to the sequence of microlayers and the Fe, Mn, Si, and Al abundance. However, the thickness and the distribution of the more soluble elements change significantly. The varnish appears to be thinner on the hamada than on the gravel at the base of the section, probably because layers were eroded on the flat surfaces. In contrast the varnish is thick and well preserved along the cliff. Calcium, P, Na, and S are concentrated at the base of the varnish in the samples (14A6 and 5A) from flat positions. In the samples from the cliff, Na and S have random distributions while a large amount of P and Ca are concentrated in microlayer 2 or at its top. Similar to the sample IHA, the more soluble elements appear to be redistributed by postdepositional processes across the varnish via percolating capillary water and evapotranspiration.

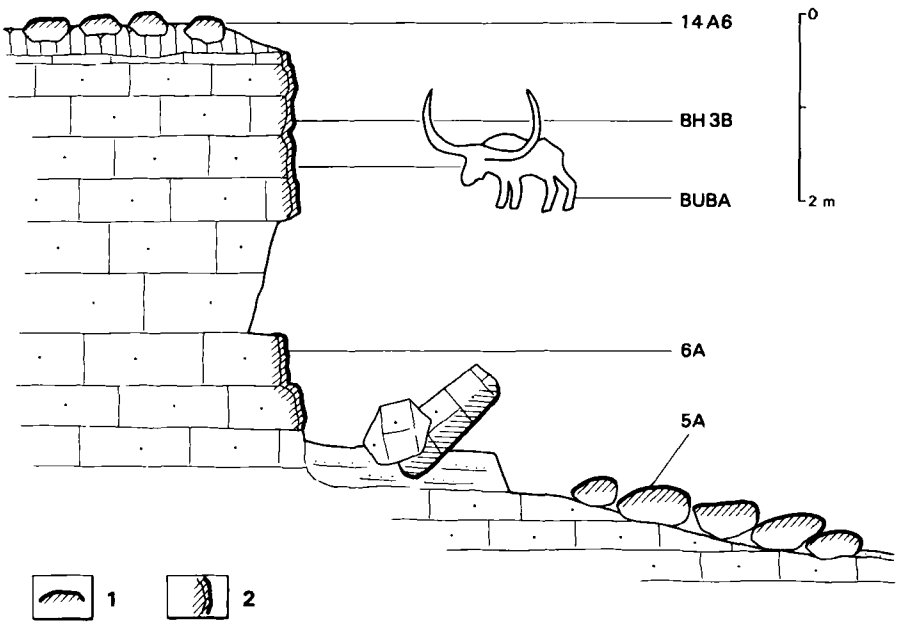

Figure 7. The toposequence at In-Habeter; location of samples: 14 A6 on the top of the plateau, BH3B, 6A and BUBA, associated with an engraved *Bubalus*, along the cliff; 5A on the gravel in the wady. **1.** Varnished surfaces; **2.** varnished surfaces underlined by the reduction rim.

The topographic position influences the thickness of the varnish and the distribution of the mobile ions Ca, P, Ba, Na, and S. In contrast, no clear correlation appears to exist between the relative age of the geomorphological units and the appearance or chemical characteristics of the varnish. The varnish displays the same sequence of microlayers and similar distribution of the more stable elements (Fe, Mn, Si, and Al) on the top of the hamada, on the cliff, and on the bar gravel, which are landforms of rather different age.

RELATIVE DATING: VARNISH AND ROCK ENGRAVINGS

The Messak Settafet is one of the areas of higher concentration of rock engravings in Central Sahara (Frobenius, 1937; Graziosi, 1938; Castiglioni and Negro, 1986; Van Albada and Van Albada, 1994; Lutz, 1995). Four main groups of petroglyphs are distinguished and dated relatively on the basis of the subjects, the technique, and superpositions of the engravings (Mori, 1965; Lothe, 1970; Hachid, 1984; Muzzolini, 1993):

- The Wild fauna group (WF) is generally related to Epipaleolithic hunters, but a later attribution to middle Holocene was proposed by Muzzolini (1986). WF represents large undomesticated mammals, mainly *Bubalus* (*Homoioceras*) *antiquus*.

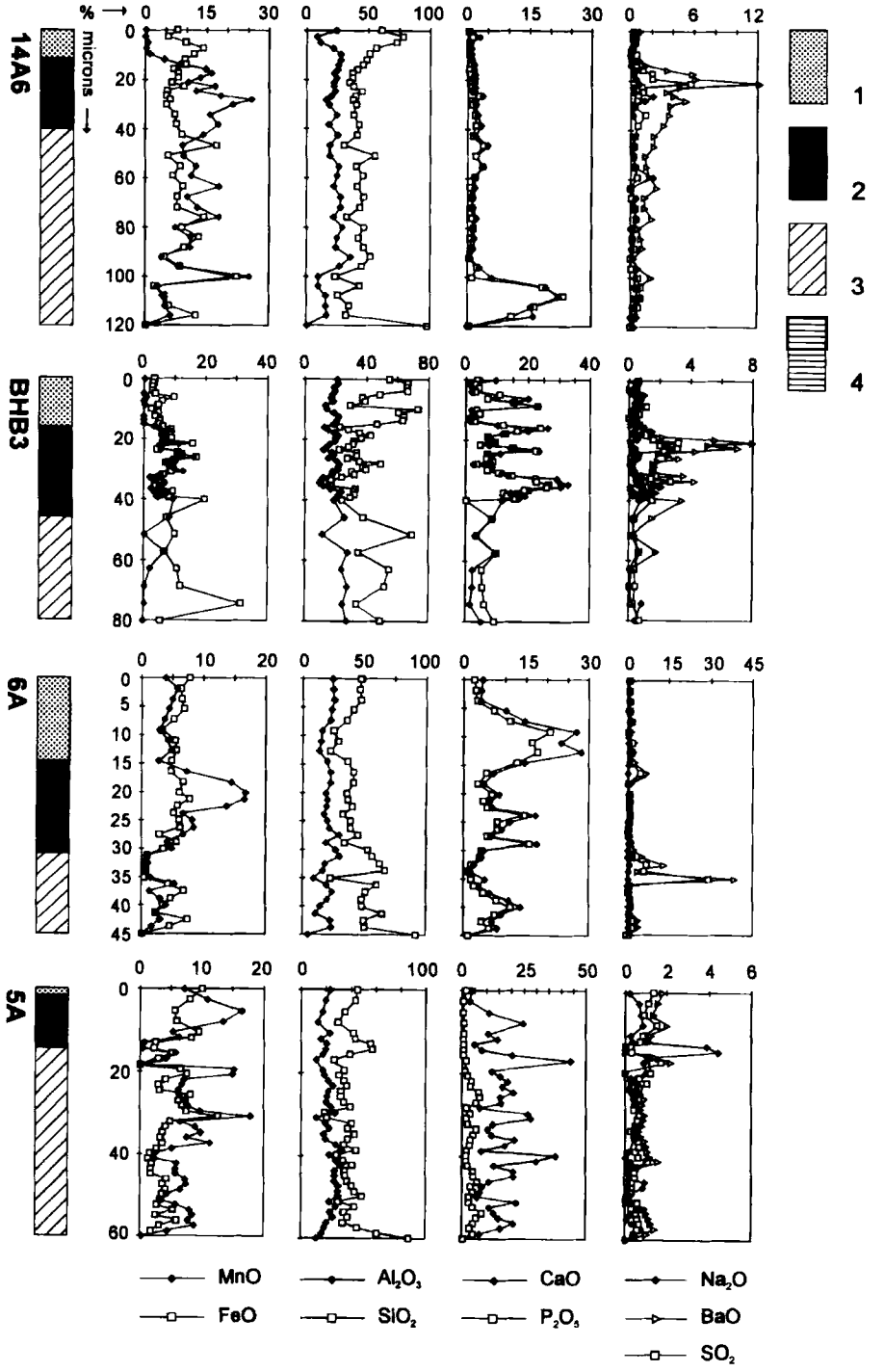

Figure 8. The chemical composition of the toposequence samples identified in Figure 7: Microlayers are indicated as follows: **1.** Microlayer 1; **2.** microlayer 2; **3.** microlayer 3; **4.** red iron-rich varnish.

- The Pastoral group consists of large wild mammals that are associated with domesticated cattle (*Bos macroceros* or *Bos brachyceros*); humans are also represented wearing masks in hunting or ritual scenes. This group is generally related to the whole Neolithic cycle. Pastoral style is further subdivided into early, middle, and late on the base of the style of the figures (Mori, 1965). In this article, however, only petroglyphs of the Early (EP) and Late Pastoral groups (LP) are examined.
- Horse group (HG): Running horses pulling a chariot and bitriangular humans are the main figures of this period, which is dated to the II millenium B.C. (Mori, 1965).
- Camel group (CG): It includes camel figures and *tifinagh* inscriptions. It is dated from about the II century B.C. to the III century A.D.

The petroglyphs have different degrees of revarnishing, especially in comparison with the varnish affecting the natural rock. This fact appears to be time-dependent, as older engravings have thicker and darker varnish than the younger ones. In order to study the development of varnish with time, the furrow of the petroglyphs can be considered as a fresh substratum of known relative age, making it possible to build a chronosequence of different stages in varnish development.

The relationship between varnish and engravings, based on hundreds of observations, appears rather constant in the whole area (Mori, 1965; Van Albada and Van Albada, 1994; Lutz, 1995). Comparing the petroglyphs on vertical cliffs, I observed that the furrows of the WF and EP engravings have the same degree of varnishing of the rock. The furrows of the WF have the same corroded aspect of the rock surface. The furrows of EP engravings, however, are sharp, deeply cut and the striations due to polishing, are evident at the macroscale. The furrows of LP engravings, on the contrary, are cut into previously varnished surfaces, but the LP furrows show a bright yellowish-red color, often much redder than the bedrock. No coatings have been observed in the HG and CG engravings that have the color of the unweathered bedrock.

A microstratigraphy for the petroglyph varnishes has been confirmed at the micro scale by observations in thin section of the furrows of selected engravings (Figures 9 and 10). The sample BUB comes from an engraving representing a *Bubalus antiquus*, of the WF group. The furrow is shallow, eroded in a fashion similar to the natural surface of the rock, and has irregular boundaries. The varnish is composed of the three microlayers as described above, displays the same stratigraphy outside and inside the furrow, and the reduction rim runs closely parallel to the surface.

Sample EL comes from a large rock engraving representing an elephant of the EP group; the furrow has a sharp boundary and a regular concave shape, with a smooth surface resulting from polishing. The stratigraphy of the varnish, both in the furrow and on the surface of the rock, is almost the same. However, the varnish is better preserved inside the furrow, and it appears to

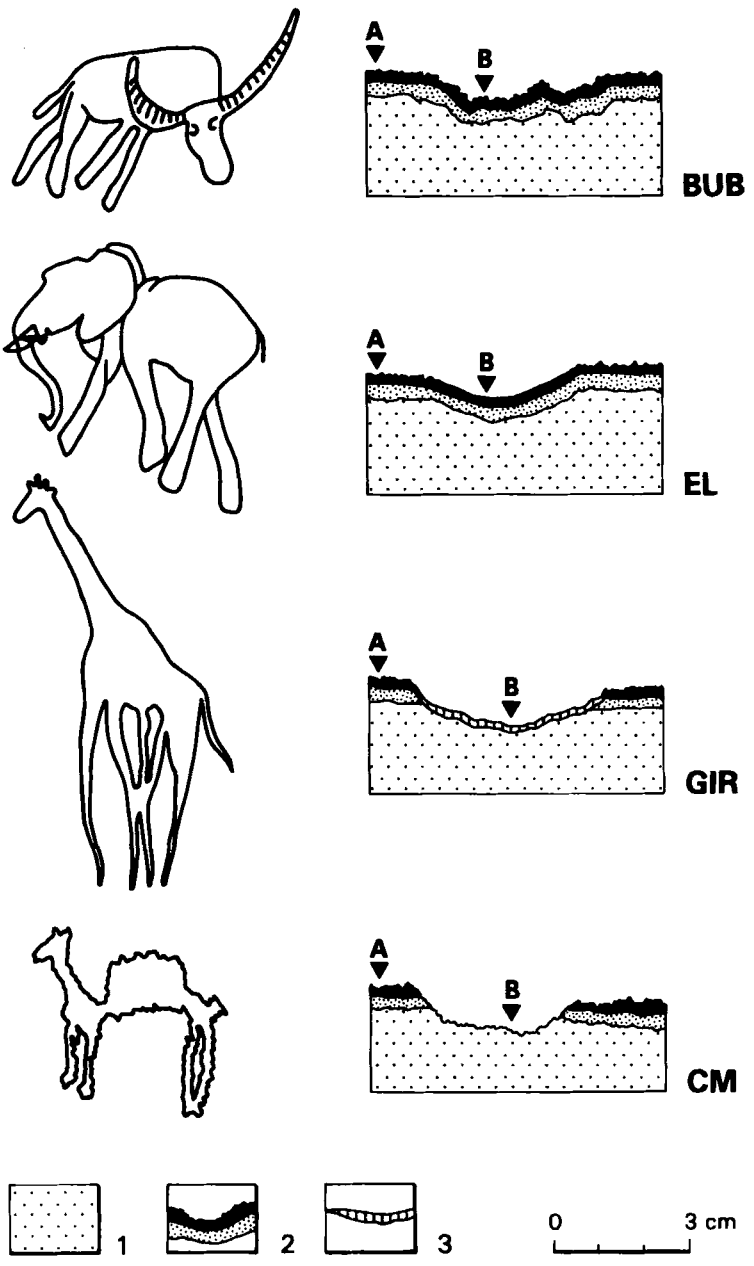

Figure 9. Cross sections of the selected engravings representing, from the top, the following styles: WF—*Bubalus*, EP—*Elephas*, LP—giraffe, late group—camel. Figures and varnish layers are not to scale: **1.** sandstone bedrock; **2.** varnish and reduction rim; **3.** red iron-rich varnish.

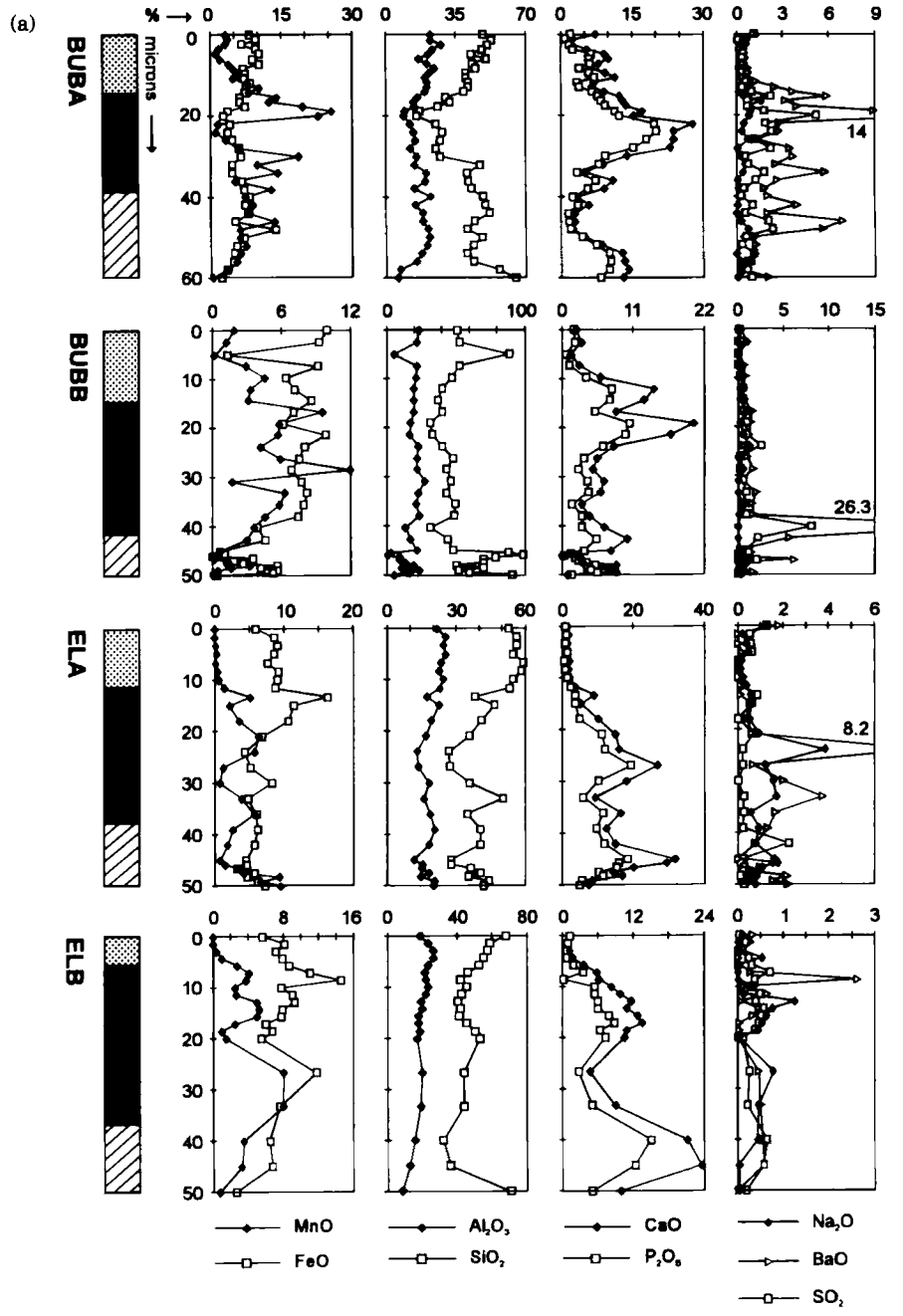

Figure 10a and 10b. Chemical composition of the varnishes on selected petroglyphs; location of the subsamples as in Figure 9; legend as in Figure 8.

(b)

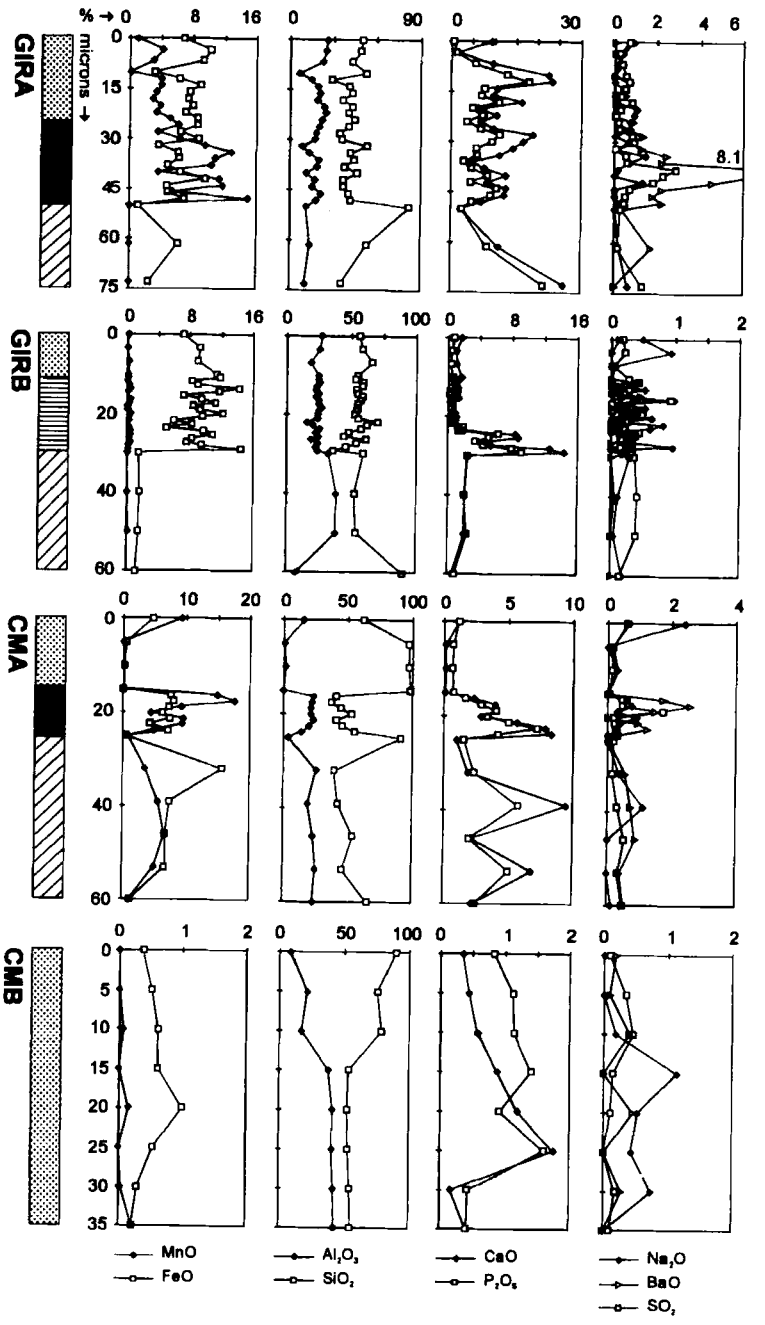

Figure 10—*Continued*

be somewhat eroded on the natural surface of the rock. Consequently, the upper microlayer (microlayer 1) of the sample inside the furrow is thicker and includes reworked varnish fragments.

The GIR sample was collected from a giraffe engraving of the LP group. The furrow looks sharp and freshly preserved. It clearly cuts both the black varnish and the reduction rim, and it is covered by a yellowish-red varnish (5YR 5/6). It consists of finely subdivided material which fills the intergranular spaces to an average depth of 40 μm. The red varnish appears homogeneous, as no laminations have been observed in it. The Mn content is very low, while Fe reaches 15%; Ca and P are well represented in the lower part. At the upper part of the coating a layer composed mainly of Si and Al is indicative of unweathered dust, which is therefore correlated with the microlayer 1 of the manganese-rich varnish.

The CM sample is representative of the Camel group. The shallow furrow has an irregular shape, as if the furrow was made by hammering. In it, the bedrock appears unweathered, and only few intergranular voids exhibit lenses of trapped dust that represents a discontinuous microlayer 1. This microlayer is mainly composed (sample CMB) of silica and aluminum indicative of unweathered clay particles. The slight peak of iron may be related to incorporation of detrital iron-rich minerals into the accumulating dust. The minor content of Ca, P, Na, and S may indicate that these elements are a part of the most recent aerosol trapped on the rock surface.

The microstratigraphy of the rock coatings on petroglyphs constrains the sequence of layering. Black desert varnish developed after the engravings of the WF and EP groups were carved.

However, before the development of the varnish, the furrows of the WF petroglyphs were subjected to a corrosion phase. Rough surface and underlying reduction rims, together with clay textural features in the lower part of the varnished surfaces, may be interpreted as the effect of weathering of the rock surface in a wet environment. In contrast, engravings of the EP group did not show any rock-surface alteration before the formation of black manganese-rich varnish. Black manganese-rich varnish has not formed in the time since the LP engravings were made; LP engravings are only coated by red iron-rich varnish.

Because no microenvironmental factors can be called upon to explain why these petroglyphs remained unvarnished, the environmental conditions conducive to the formation of manganese-rich black varnish must have come to an end before the manufacturing of the LP engravings.

THE AGE OF THE MANGANESE-RICH VARNISH

Significant archaeological evidence constraining the period of development of the manganese-rich varnish has been discovered in two archaeological sites. One is located a short distance from In-Habeter (25°43′06″N; 12°11′29″E) while the other is in wadi Tilizzagen (25°47′56″N: 11°54′33″E).

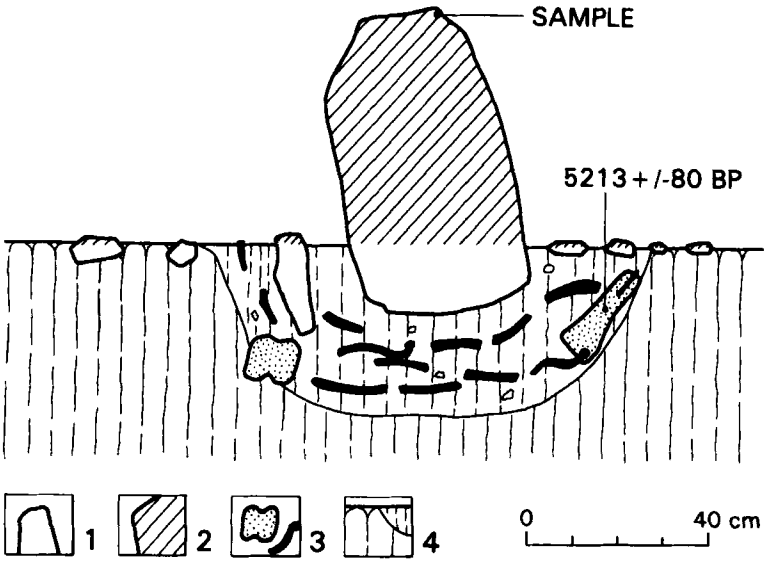

Figure 11. The In-Habeter stele: the stele covers a pit including Neolithic pottery and burned bones: **1.** stones; **2.** varnished surfaces; **3.** bones and sherds; **4.** soil and pit.

In the In-Habeter site, a votive stele (Figure 11) was erected over a small pit which contained Neolithic pottery and burned bones radiocarbon-dated to 5213 ± 80 yr B.P. (GX-19108-AMS). Only the part of the stele and pottery fragments that stick out from the ground are covered by the black manganese-rich varnish (Figure 12). The buried parts of both stele and pottery fragments are uncoated. The radiocarbon age represents a minimum for the development of the manganese-rich varnish as, on the stele, the varnish developed after this data. It seems a reasonable assumption that the stele was uncoated when erected, as the pottery fragments certainly were when they were thrown into the pit. The varnish on the stele is quite black, and rich in iron and manganese. As the sample was collected in a location exposed to rain showers, the Ca and P are leached at the base of microlayer 2, similar to that in sample 14A6 of the toposequence. However, microlayer 3 is poorly developed; no illuvial clay and reduction rim were detected below the black varnish.

At Wadi Tilizzaghen (Figure 1), an archaeological megalithic structure was excavated. It is composed of a circle of standing stones delimiting an artificial fill of sand and gravel. The structure also includes a small hearth at its base whose charcoal yielded a radiocarbon age of 4915 ± 79 yr B.P. (GX-19827-AMS). Only the part of the megalith stones that sticks out of the ground is coated by the Mn-rich black varnish. As the varnish formed after the structure was built, the ^{14}C age indicates that the varnish was still forming at the beginning of the V millennium B.P.

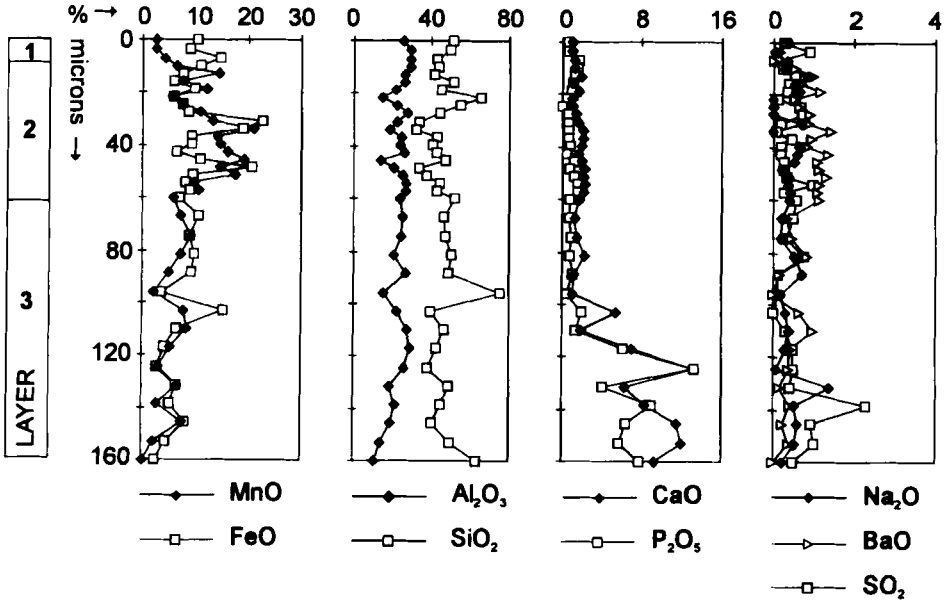

Figure 12. The chemical composition of the varnish stratigraphy on the stele sample.

At In-Habeter, 100 m north of the stele mentioned above, a cairn was excavated, composed of several stratigraphic units (Figure 13). At the top there is a large stone heap (US1, US2), covering artificially accumulated sand (US3, US4). At the base of the section there is a skeleton surrounded by stones (US5). Charcoal fragments, from US4, yielded a radiocarbon age of 5071 ± 91 yr B.P. (GX-20348 AMS). The cairn has been built in part on a clayey soil and in part on a sandstone outcrop. Both the stones at the top of the upper unit (US1) of the cairn and the surface of the sandstone on which the cairn lies are coated by black manganese-rich desert varnish (Figure 14). The upper sample (MT 132A) was obtained from a block that exhibited varnish only on the side exposed to the surface. Therefore, the block had been put on the cairn while still unvarnished, and the varnish had developed only since the cairn was finished. The varnish in the upper sample (MT 132A) (Figure 14) is mainly represented by microlayers 1 and 2, both particularly thin; in microlayer 2, which displays typical lamination, Mn prevails over the iron. As in every sample connected to a flat surface, Na and S are leached in the lowermost microlayer, which is very thin.

The lower sample (MT 131) (Figure 14) was exposed to varnish formation only before the construction of the cairn. Its microlayer 2 is much thicker than the upper one and displays the typical lenticular lamination. At its base, microlayer 3 is strongly developed and a reduction rim occurs 5 mm deep from the surface. Microlayer 1 is lacking and microlayer 2 is sealed by a thin calcium

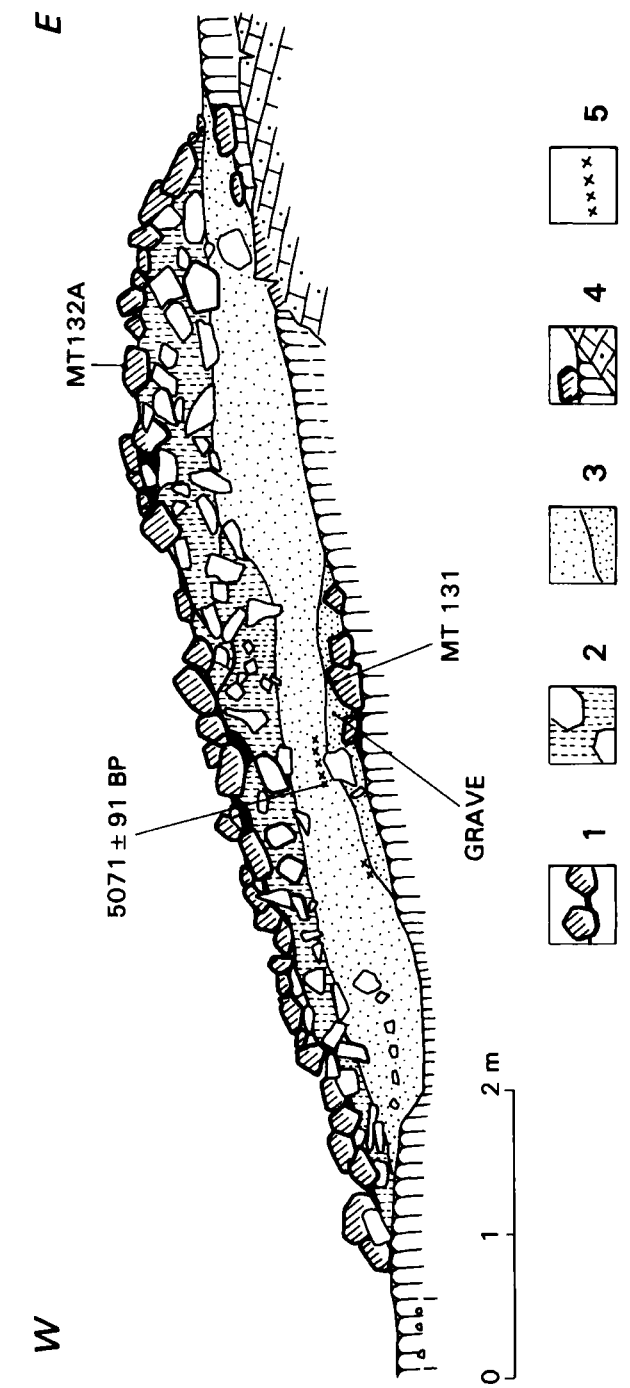

Figure 13. The In-Habeter cairn: cross section. The cairn, including a grave at its base, was erected on a varnished surface: **1.** heap of stones (US1 and US2); **2.** stones and sand US3; **3.** accumulated sand (US3 and US4); **4.** base soil, base stones and sandstone outcrops; **5.** charcoal fragments.

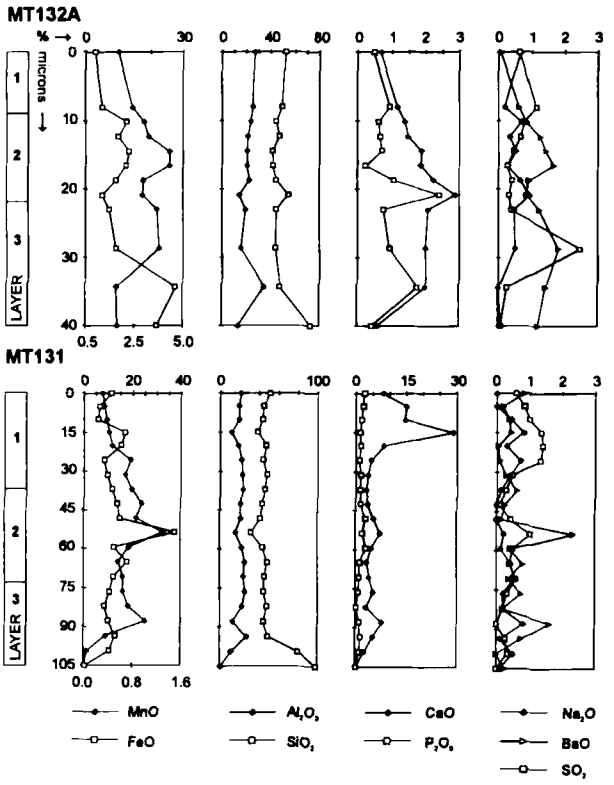

Figure 14. The chemical characteristics of the varnish stratigraphy from samples MT132A and MT131 from the In-Habeter cairn.

carbonate concretion, probably due to percolating water. In this carbonate concretion, a relevant amount of S and Na occurs and indicates that gypsum and halite were originally included in the sand units of the cairn (US2–US5) from which they have been removed by leaching and deposited on the underlying varnish-coated surface.

The In-Habeter site provides an opportunity to understand varnish development on the surface and subsurface after a given known age. Comparing the degree of development of the two samples of varnish, one on the top and the other at the base of the cairn, I conclude that the varnish was already developing when the cairn was built and it continued to develop in a subaerial location, on the top of the cairn (sample MT 132A), and when the construction of the cairn was finished. However, the development of the black, manganese-rich varnish of the upper sample (MT 132A) did not last long enough to reach the thickness of the varnish in the surface buried by the cairn construction (sample MT 131). The accumulation of the varnish is, therefore, a progressive process,

and at the time of the construction of the cairn it was in the late phase of its formation.

Sample MT 131 should be regarded as being representative of the general situation at least at the In-Habeter site. In the vicinity of the stele, a large Neolithic workshop was uncovered (Di Lernia et al., 1995) lying upon a varnished sandstone surface, sealed by carbonate concretion and buried by an alkaline sandy soil.

The sample MT 131 also indicates that the varnish can survive when buried in alkaline soil, and therefore it supports the fact that the varnish was not on the stele and on the Tilizzaghen megalith when they were built; otherwise, remnants of varnish would have to be found below the present surface.

THE PALEOENVIRONMENTAL CONTEXT

A consistent reconstruction of the environmental conditions conducive to varnish deposition requires correlation with contemporary and independent paleoclimatic data. These data were obtained from the study of the fill of the Matendush cave (25°42′41″N; 12°05′25″E) located close to the varnish-sampling sites (Lutz, 1992; Cremaschi, 1994). The fill of the cave is composed of the following stratigraphic units from top to bottom (Figure 15). A dung layer (US0), dated 4565 ± 165 yr B.P. (GX-17797), overlies archaeological levels including hearths, nonhumidified plant remains, and late Neolithic artifacts (US2). The units US3 and US4 follow and are composed of sand and humified organic material, including scarce archeological material. Radiocarbon dating of charcoal in US4 yielded an age of 6825 ± 90 yr B.P. (GX-17797).

Pollen counts (Trevisan et al., 1993) (Figure 15) show that the US4 and US5 units are indicative of a wet savanna climate, as they are characterized by hygrophylous grass (*Cyperaceae*, *Typha*, and *Lithisum*), and by some allocthonous tree pollen (*Pinus*, *Quercus*) from the upper reaches of the plateau. Only very few arid species (*Ramarix*, *Capperaceae*, and *Compositae*), which rise slightly in US3, were recorded at the USS 4/5 level. Units US0–US2 are rather different as the most common species belongs to herbaceous nonhydrophilous plants of dry savanna-type vegetation (*Echium*, *Maerua*, *Cruciferae*, *Leguminosae*, and *Compositae*).

Based on the radiocarbon ages, the dry steppe environment appears to be contemporary with the formation of the manganese-rich black varnish, which therefore meets the climatic requirements indicated by Dorn (1990, 1994) as favorable for the life of the manganese-fixing bacteria. The wet conditions present at the base of the cave fill, dating to the VIIth millennium B.P., could correlate with the formation of the lowermost microlayer 3 in the varnish. Aeolian sand at the top of the sequence (US1) indicates dry conditions.

DISCUSSION OF VARNISH STRATIGRAPHY

Eolian input on rock surfaces, incidentally redistributed by occasional rain showers, is the main process that provided the raw material for the development

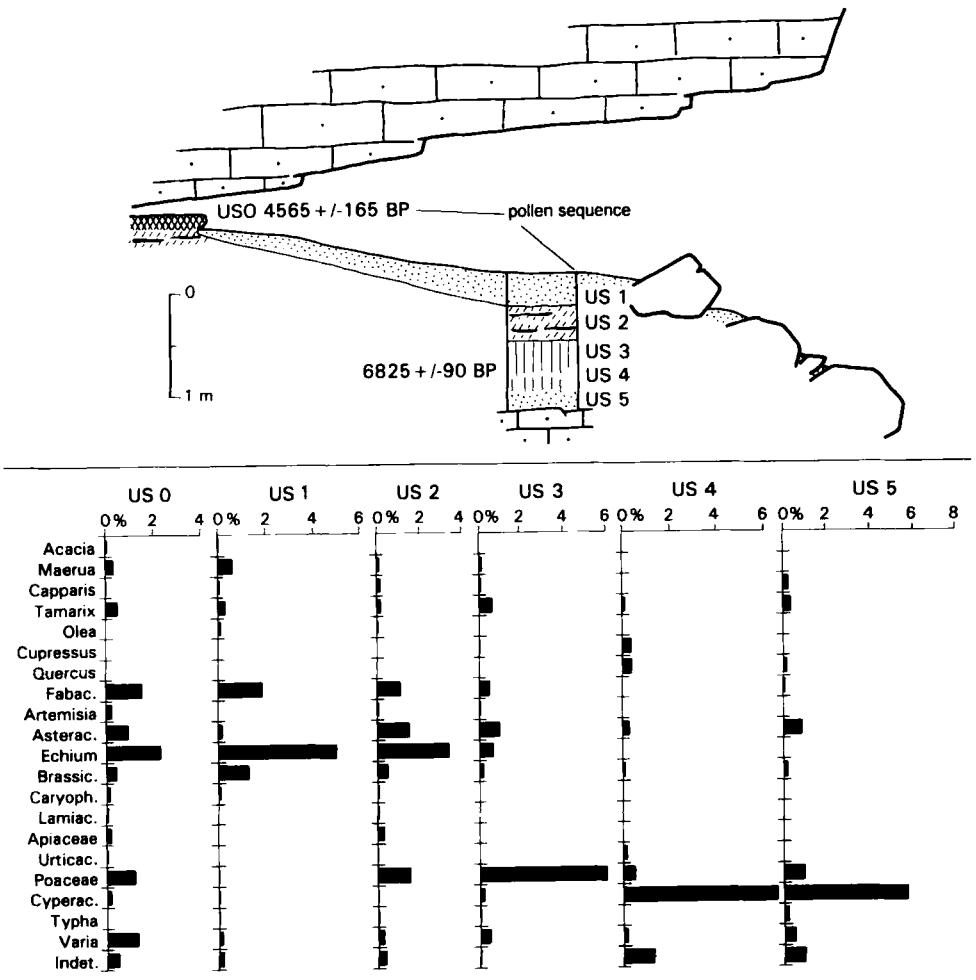

Figure 15. The Matendush cave and its pollen diagram. The fill of the cave is composed at the base by sterile sand (US5); US2–hearth, US3 and US4 are rich in organic matter and includes Neolithic artifacts; US0 is constituted by consolidated dung and US1 by wind-blown sand.

of the varnish. However, the texture and lithology of the substrate also plays an important role, as the roughness of the surface of the sandstone outcrops acts as a trap for the aerosols.

The three different microlayers that are characteristic for the Messak Settafet varnish result from processes acting at different times and in different environments. Illuvial clay and a reduction rim in the innermost microlayer (microlayer 3) are indicative of wet climatic conditions. In fact, translocation of clay in a dispersed state requires slightly acidic pH and alternating cycles of wetting and drying; similar conditions are needed for the formation of rube-

fied iron hydroxides. The reduction rim is interpreted to result from capillary water penetrating the rock and weathering the outer layer of rock; this is consistent with its friable nature and its discoloration.

The innermost microlayer and the related reduction rim are discontinuous and are unconformably overlain by the upper two microlayers. The innermost layer is preserved in the most stable parts of the landscape, as on the In-Habeter cliff, below the furrow of the WF engravings and in the In-Habeter bedrock of the In-Habeter cairn. The reduction rim is absent, and the lowermost layer is poorly developed in more recently exposed surfaces, such as the furrows of Pastoral engravings of the stele and the top stone of the cairn, which have been exposed only since the V millennium B.P. Consequently, clay coatings in microlayer 3 and the reduction rim should be considered as relict features, predating the deposition of the manganese-rich black varnish.

The microlayer 2, indeed, corresponds to the typical rock varnish, as described in the literature. An upward increasing trend in Mn accumulation and an abrupt upper boundary can be observed in many samples, indicating that conditions conducive to manganese accumulation developed gradually and ended suddenly. Frequent occurrence in this microlayer of P and Ca should be interpreted as relating to biological activity, indicative of the persistence of some wetness in the environment.

The upper, outer microlayer is composed of quartz dust and clay minerals that did not undergo chemical or biochemical alteration; it is therefore indicative of a dry environment. Lithorelicts of the varnish, however, are included in this microlayer, which often shows convolute laminated fabric; both features indicate erosion and redeposition induced by episodic rain showers. Minor occurrences of alkaline elements in the outer layer may indicate deposition after drying of the lakes located in the erg.

The geomorphological evidence (varnish with the same characteristics covers both recent and old landforms) and the varnish associated with engravings (the varnish developed after the WF and EP petroglyphs were engraved) indicates that the varnish was formed during the Holocene. No varnish outcrops older than the Holocene have been found in the Messak Settafet at present, while, to the contrary, in many other desert areas (Dorn, 1994) varnish formation started well back in the Pleistocene. This lack is due to climatic changes, ranging from wet savanna to hyperarid conditions, which affected the central Sahara since the Middle Pleistocene (Vernet, 1994). Cyclic shifts in the environment enhanced the rejuvenation of geomorphological surfaces and therefore led to varnish destruction.

Radiocarbon-dated archaeological evidence indicates that, in the Messak, the manganese-rich varnish began to form in the late VI millennium B.P. or at the beginning of the V millennium B.P., in a dry steppe environment. The ecological conditions conducive to varnish formation ceased to exist by the time the LP engravings were made and the red varnish developed is typical of dry conditions (Oberlander, 1994). Full desert conditions are further indicated by

microlayer 1 of the varnish and by the uncoated furrows of the HG and CG engravings. The beginning of the arid phase, which stopped the formation of the Mn-rich varnish, cannot be dated directly. The cessation probably corresponds to the drying of the ponds and lakes surrounding the mountain ranges, which in the central-western Sahara are dated to around the IV millennium B.P. (Petit Maire and Riser, 1983; Cremaschi, 1992; Di Lernia and Cremaschi, in press).

CONCLUSION

The microlayering of varnish in the central Messak Settafett suggests that varnish formation was complex and went through a progressive shift from wet environmental conditions towards aridity. The microlayering consists of the following sequence. The lowermost microlayer is discontinuous and appears to have been originated by weathering of the sandstone and impregnation of illuvial clay in wetter conditions than today's.

The typical desert varnish, rich in iron and manganese, as described in the literature, only corresponds to microlayer 2. It started to develop during the time span from the end of the VI to the beginning of the V millennium B.P., as indicated by its occurrence on the radiocarbon-dated archaeological monuments at In-Habeter and Tilizzagen. The black varnish seals the WF and EP engravings which were therefore made before deposition of the varnish.

Comparison with the local pollen record suggests that the black varnish was formed in a dry steppe environment, and therefore in conditions of moderate dryness, in perfect accordance with the biochemical model proposed by Dorn (1990, 1994).

At the time of Late Pastoral engravings, the black varnish was not forming as these petroglyphs were covered by iron-rich coatings that are typical of those formed in a dry environment. The upper microlayer, composed of unweathered dust, covers both black varnish and the red coating and indicates the onset of full desert conditions in the area. At present this phase cannot be dated accurately, but should be referred to the IV millennium B.P.

Today, the formation of varnish is no longer active, or it is slower than degradational processes. The surfaces on which varnish developed are gradually being destroyed by gravitational collapse and wind erosion.

The research on the Messak rock varnish was conducted in the frame of the Italo-Libyan archaeological mission directed by F. Mori. The author is grateful to F. Mori for encouragement to undertake the research and for help in identifying the petroglyphs and to R. I. Dorn for many suggestions in the review of the manuscript. The author thanks the whole Italian and Libyan staff for assistance and cooperation. The author is deeply indebted to R. Lutz and G. Lutz, A. Van Albada, and S. Di Lernia for discussion, and to A. Rizzi for technical assistance with the SEM.

REFERENCES

Allen, C.C. (1978). Desert Varnish of the Sonorian Desert—Optical and Electron Probe Microanalysis. *Journal of Geology* **86**, 743–752.

Bullock, P., Fedoroff, N., Jongerius, A., Stoops, G., Tursina, T., and Babel, C. (1985). *Handbook for Thin Section Description.* Albrighton, U.K.: Waine Research.

Busche, D. (1980). On the Origin of the Msak Mallat and Hamadat Manghini escarpements. *In* M.G. Salem and S. Busrewil, Eds., *The Geology of Libya*, pp. 837–848. Amsterdam: Elsevier.

Castiglioni, A., and Negro, G. (1986). *Fiumi di Pietra. Archivio della Preistoria Sahariana.* Varese: Lativia.

Cooke, R.U., Warren, A., and Goudie, A. (1993). *Desert Geomorphology.* London: UCL Press.

Coudé-Gaussen, G. (1991). *Les Poussieres Sahariennes.* Montrouge, London, Rome: John Libbey Eurotext.

Cremaschi, M. (1992). Genesi e Significato Ambientale della Patina o Vernice del Deserto e Suo Ruolo nello Studio dell'Arte Rupestre. II Caso del Fezzan Meridionale (Libya). *In* M. Lupacciolu, Ed., *Arte e Culture del Sahara Preistorico* pp. 77–87. Rome: Quasar.

Cremaschi, M. (1994). Le Paleo-Environment du Tertiaire Tardif à l'Holocène. *In* A. Van Albada and A.M. Van Albada, Eds., *Art Rupestre du Sahara*, pp. 4–14. Les Dossiers d'Archeologie **197.** Quetigny:SFBD/ARCHEOLOGIA SA.

Di Lernia, S., and Cremaschi, M. (in press). Climatic Changes and Human Adaptive Strategies in the Central Saharian Massifs: The Tadrart Acacus and Messak Settafet Perspectives (Fezzan, Libya). *In Proceedings of the 10th Pan-African Congress*, Harare, 1995, June 14–18.

Di Lernia, S., Cremaschi, M., Biola, S., Merighi, F. and Sivilli, S. (1995). Processing Quarzite in Central Sahara: A Case Study from In Habeter III Wadi Mathendusch (Messak Settafet, Libya). Abstracts of the VIIth International Flint Symposium, Ostrowiec: Institute of Archaeology and Ethnology, Polish Academy of Science, September 4–8, pp. 15–16.

Dorn, R.I. (1984). Cause and Implications of Rock Varnish Microchemical Laminations. *Nature* **310,** 767–770.

Dorn, R.I. (1990). Quaternary Alkalinity Fluctuations Recorded in Rock Varnish Microlaminations on Western U.S.A. Volcanics. *Paleo, Paleo, Paleo* **76,** 291–310.

Dorn, R.I. (1994). Rock Varnish as Evidence of Climatic Change. *In* A.D. Abrahams and A.J. Parsons, Eds., *Geomorphology of Desert Environments*, pp. 539–552. London: Chapman and Hall.

Dorn, R.I., and Oberlander, T.M. (1981a). Rock Varnish Origin, Characteristics and Usage. *Zeitschrift für Geomorphologie* **25**(4), 420–436.

Dorn, R.I., and Oberlander, T.M. (1981b). Microbial Origin of Desert Varnish. *Science* **213,** 1245–1247.

Frobenius, L. (1937). *Ekade Ektab. Die Felsbilder Fezzans.* Liepzig: Harrassowitz.

Graziosi, P. (1942). *L'Arte Rupestre della Libia.* Napoli: Mostra d'Oltremare.

Hachid, M. (1984). La Chronologie Relative des Gravures Rupestres de l'Atlas Saharien (Algerie) et la Region de Djelfa. *Bulletin de la Societè Prehistorique Francaise* **81**(2), 143–164.

Jelinek, J. (1985). Tilizahren, the Key Site of the Fezzanese Rock Art. *Anthropologie* **33**(3), 262.

Jones, C.E. (1991). Characteristics and Origin of Rock Varnish from the Hyperarid Coastal Deserts of Northern Peru. *Quaternary Research* **35,** 116–129.

Krinsley, D.H., Dorn, R.I., and Anderson S.W. (1990). Factors That Interfere with the Age Determination of Rock Varnish. *Physical Geography* **11,** 97–119.

Lothe, H. (1970). Gravures Rupestres de Tin-Terirt, Iherir, Aharar Mellen, Amsedenet et In Tebourbouga. *Libyca* **18,** 185–234.

Lutz, R.G. (1992). Grotte e Ripari nell'Amsach Settafet (Fezzan, Libia). *Sahara* **4,** 130–134.

Lutz, R.G. (1995). *The Secret of the Desert. The Rock Art of Messak Settafet and Messak Mellet, Libya.* Innsbruck: Golf Verlag.

Mori, F. (1965). *Tadrat Acacus, Arte Rupestre e Culture del Sahara Preistorico.* Rome: Einaudi.

Muzzolini, A. (1986). *L'Art Rupestre Préhistorique des Massifs Centraux Sahariens.* B.A.R. International Series 318. Oxford: British Archaeological Reports.

Muzzolini, A. (1993). Chronologie Raisonnée des Diverse écoles d'Art Rupestre du Sahara Central. *In* G. Calegari, Ed., L'Arte e l'Ambiente del Sahara Preistorico: Dati ed Interpretazioni. *Memorie*

della Società Italiana di Scienze Naturali e del Museo Civico di Storia Naturale di Milano **26**(II), 387–397.

Oberlander, T.M. (1994). Rock Varnish in Deserts. *In* A.D. Abrahams and A.J. Parsons, Eds., *Geomorphology of Desert Environments*, pp. 107–119. London: Chapman and Hall.

Petit Maire, N., and Riser, J. (1983). *Sahara ou Sahel. Quaternaire Récent du Basin des Taoudenni (Mali)*. Marseille: Laboratoire de Géologie du Quaternaire.

Potter, R.M., and Rossman G.R. (1977). Desert Varnish: The Importance of Clay Minerals. *Science* **196**, 1446–1448.

Reneau, S.L., Raymond, R., and Harrington, C.D. (1992). Elemental Relationships in Rock Varnish Stratigraphic Layers, Cima Volcanic Field, California, Implications for Narnish Development and the Interpretation of Varnish Chemistry. *American Journal of Science* **292**, 684–723.

Syers, J.K., and Iskandar, I.K. (1973). Pedogenetic Significance of Lichens. *In* V. Ahmadjian and M.E. Hale, Eds., *The Lichens*, pp. 225–248. New York: Academic Press.

Trevisan, G., Mercuri, A., and Cremaschi, M. (1993). Palinology and Stratigraphy of Deposits of the Wadi Aramas Cave (Messak Settafet, Libyan Sahara). *Giornale Botanico Italiano* **127**(3), 167.

Van Albada, A., and Van Albada, A.M. (1994). *Art Rupestre du Sahara*. Les Dossiers d'Archeologie **197**. Quetigny: SFBD/ARCHEOLOGIA SA.

Vernet, R. (1994) *Les Paleoenvironnements du Nord de l'Afrique depuis 600.000 Ans*. Dossiers et Recherches sur l'Afrique 3, UPR 311. Meudon: C.N.R.S.

Walter, H., and Lieth, H. (1960). *Klimadiagramm, Weltatlas*. Jena: G. Fisher.

Received April 5, 1996
Accepted for publication June 3, 1996